sustainability

MDPI

Article

The Robustness of Battery Electric Bus Transit Networks under Charging Infrastructure Disruptions

Hatem Abdelaty [1], Ahmed Foda [1,2] and Moataz Mohamed [1,*]

[1] Department of Civil Engineering, McMaster University, Hamilton, ON L8S 4L8, Canada
[2] Department of Mathematics & Engineering Physics, Mansoura University, Mansoura 35516, Egypt
* Correspondence: mmohame@mcmaster.ca

Abstract: The optimization of battery electric buses (BEBs) systems in transit is receiving considerable scholarly and practical attention. The practice is to minimize the total system cost to inform the optimal resource allocation. However, a minimization approach is insensitive to assessing and accommodating the robustness of BEB transit systems under disruption. This study evaluates the robustness of the BEB transit system under charging infrastructure disruption using complex network theory. The results of a mid-size multi-hub network indicate that the BEB system is robust against disruption if the disruption is resolved in a timely manner (within one hour). Furthermore, multi-charger charging stations have severe impacts on the system's robustness. Overall, the BEB system robustness is more sensitive to the hourly number of buses charging at each station and the duration of the charging events.

Keywords: battery electric buses; robustness; disruption; cascading impact; optimization; sensitivity

check for updates

Citation: Abdelaty, H.; Foda, A.; Mohamed, M. The Robustness of Battery Electric Bus Transit Networks under Charging Infrastructure Disruptions. *Sustainability* **2023**, *15*, 3642. https://doi.org/10.3390/su15043642

Academic Editor: Armando Cartenì

Received: 19 January 2023
Revised: 6 February 2023
Accepted: 10 February 2023
Published: 16 February 2023

1. Introduction

The relevance of incorporating electric drive technologies into public transit networks is expanding to mitigate transportation-related greenhouse gas (GHG) emissions and improve energy efficiency. This motivated several cities to adopt alternative-fuel buses, particularly electric buses (e-Buses), in the transit sector. E-Buses have long been seen as a viable option to substitute conventional internal combustion engine (ICE) buses due to their enhanced operation performance, noise reduction, and reduced operational costs [1,2]. Furthermore, e-Buses promise significant GHG reductions per passenger kilometer traveled, even if the electricity is not 100% carbon-free [3].

In general, e-Buses are categorized into three main types: Fuel Cell e-Bus (FCEB), which generates onboard electricity from fuel cells; Trolly e-Bus, which utilizes overhead wires that supply the electric motor with the energy continuously; and Battery e-Bus (BEB), which stores the energy on onboard batteries to power the electric motor [4]. The latter is considered more economically feasible as it enables the optimal utilization of the charging process during dwelling times. Moreover, compared to BEB, FCEB faces various practical challenges due to the lack of global technical regulations for hydrogen vehicles. Also, Trolley e-Buses require an extensive overhead-wiring infrastructure system [4].

That said, the utilization of BEBs in transit necessitates robust infrastructure planning and optimization, where each bus route must have a compatible charging scheme to ensure BEB's adherence to the operating schedule. However, before phasing out fuel buses, it is vital for decision-makers and transit agencies to comprehend the implications of an all-electric bus fleet on the energy infrastructure [5–8].

Towards that end, previous BEB research has been carried out across three broad domains: (1) BEB components, including the motor, battery, and auxiliary systems that determine the energy consumption rates [9–11]. Typically, this research domain is tied to advancing BEB design, and its practical implications are geared toward bus manufacturers.

(2) Charging infrastructure, including energy storage systems (ESS), charger's capacity, the number of chargers, and their spatial distribution. This domain targets the optimal spatiotemporal allocation of BEB infrastructure to satisfy the energy demand/utilization [12,13]. These studies implement two approaches to charging BEBs: en-route and overnight. (3) Bus transit network modifications, which involve altering bus routes, location of bus stops, and transfer stations in favor of electrification [14,15].

Together, these domains are addressed using advanced optimization models, which aim at minimizing the total costs of adopting BEBs systems while mitigating their external impacts (e.g., on the utility grid and GHG emissions). Furthermore, previous work also considered the optimal operational feasibility, namely, operational features such as energy consumption, charging time, availability of chargers, and state of charge (SoC) [1,16,17]; economic features such as the costs of charging infrastructure, operation, maintenance, vehicle, and battery [18–20]; and environmental features including GHG emissions and the air quality [21,22].

Despite the plethora of well-established optimization models in the BEB literature, almost all these models are based on a minimization cost function, meaning that the BEB system configuration is designed without any redundancy. However, recent optimization approaches in BEB transit network configuration address this issue by accommodating the uncertainty related to transit operation and energy demand/supply. These uncertainties are often associated with energy consumption [23–25], arrival delay to charging stations [26], and power supply variability [27]. Acknowledging the systemic uncertainty is indeed essential to offer practical solutions for the adoption of BEBs in transit. However, the scope of these studies focuses on designing the optimal BEB transit system that accommodates these uncertainties yet not measuring the impacts of disruptions on the system's performance.

As such, there is a clear gap in understanding and assessing the behavior of the BEB transit system during disruption (e.g., electricity outage or equipment malfunction), which has been recently documented [28]. Furthermore, the cascading impacts of disruption on the BEB transit network operation are still unknown. One can argue for the dire need to quantify the vulnerability of the BEB transit system to accurately design an optimal BEB system configuration.

Put another way, the works of [29–31] documented the vulnerability of transit networks (using ICE buses) to disruption. In this context, vulnerability indicates the ability of the BEB transit network to operate under the cascading failure resulting from a disruption in the network. In this context of BEB, additional disruptions could take place due to an electricity outage at any point in the utility grid or a malfunction in any of the system components (chargers).

Toward that end, this study aims to address two research questions:

(Q1) What is the robustness of BEB transit networks under disruptive events such as electricity outages or equipment malfunction?

(Q2) Which charging profile parameters have significant impacts on the robustness of BEB transit systems?

In the context of this study, we follow [32] in their definition of robustness is defined as the system's ability to maintain the desired level of service despite disruption. In this study, transit system robustness refers to the ability of the transit system to deliver scheduled trips. As such, robustness is measured using a service frequency indicator (detailed in Section 3).

Overall, addressing these three research questions brings three substantial contributions to the BEB research:

- First, we quantify the robustness of a BEB transit network using complex network theory.
- Second, we analyze the sensitivity of the BEB service robustness to several operational parameters.
- Lastly, this is the first attempt to evaluate the robustness of BEB transit system networks using complex network theory, offering some new insights into the design, planning, and optimization of BEB transit networks.

Following this introduction, a literature review of the current BEB optimization studies is discussed in Section 2. Section 3 presents the methodology, including the optimization model and the proposed complex network theory model. Section 4 describes the case study. Section 5 discusses the results, optimization, and robustness. Section 6 explains the sensitivity analysis results. While section seven discusses the findings and presents the concluding remarks.

2. Literature Review

The state-of-the-art for optimizing BEB transit system configurations, along with the associated infrastructure and the charging profile, focuses on optimizing the system costs. That is to minimize the total cost of ownership (TCO) associated with the implementation of BEB fleets in transit networks through the optimal allocation of resources. Previous studies related to BEB system configuration optimization are categorized into three groups; cost, utility impact, and GHG remissions, as listed in Table 1.

Table 1. Recent BEB system configuration optimization studies.

Author	Objective Functions (Minimize)			BEB System Configuration
	Cost	Utility Impact	GHG Emission	
Li [33]	✓			Number of chargers
Xiong [1]	✓			Number of chargers
Benoliel [34]	✓			Number of chargers & Fleet size
Liu [12]	✓			Number of chargers & Chargers' power
Uslu and Kaya [17]	✓			Number of chargers
Wu [35]	✓	✓		Number of chargers & Fleet size
El-Taweel [6]	✓	✓		Battery capacity, number of chargers & power
Lotfi [36]	✓			Battery capacity & Chargers' power
He [2]	✓			Battery capacity & Chargers' power
Lin [37]	✓	✓	✓	Number of chargers
Lin [37]	✓	✓		Number of chargers
Liu [7]	✓			Battery capacity & Chargers' power
Bi [22]	✓		✓	Battery capacity & Number of chargers
Rogge [8]	✓			Number of chargers & Fleet size
Kunith [19]	✓			Battery capacity
Wang [38]	✓			Number of chargers

Cost optimization models, where the main aim is to minimize the TCO of the BEB system, considering the number of chargers, their locations, and the charging schemes that fulfill the transit schedules limits [1,8,17,33,34,38]. Furthermore, various studies developed optimization models for fast-charging infrastructure system that minimizes the system cost by reaching the optimal battery size for each bus and their charger-rated power [2,7,12,19,36].

In comparison, cost-utility optimization models aim to minimize the operational cost and the impact on the utility grid [37]. Moreover, spatial optimization models are proposed to quantify the number of chargers required for a BEB fleet to minimize construction, operational and maintenance costs [35]. At the same time, cost-emission optimization models aim at minimizing the BEB system cost and the life-cycle GHG emissions for both the operation stage and the end-of-life stage [22].

Another distinct stream of research accommodates the uncertainty of BEB operation through the utilization of Robust and Two-stage Stochastic optimization approaches), such as the works of [13,24–26,39–42]. This approach considers the uncertainty associated with several parameters, as detailed in Table 2. The advantages of the two-stage stochastic and the robust optimization models are their ability (1) to design the system for the worst-case scenario and (2) to accommodate the uncertainty distribution of several parameters at the same time. However, their limitations, with respect to the scope of this study, are the inability to assess the robustness of the BEB system under disruptive events. The latter is the main aim of the present paper.

Table 2. BEB optimization studies with uncertainty.

Author	Robust and Two-Stage Stochastic Optimization				
	Energy Consumption	Travel Time	Charging Time	Passenger Load (Mass)	Charging Demand
Liu [24]	✓				
Zheng [26]			✓		
Zhou [40]	✓				
Bie [39]	✓	✓			
Hu [42]		✓		✓	
Jiang [41]		✓			
An [13]					✓
Liu [25]	✓				

Overall, the literature adopts optimization models for BEB relying on a minimization function of the system cost, utility impact, and component sizing. However, a minimization function is not ideal for BEB system configuration, especially when challenged with disruption events (e.g., power outage) [43]. Indeed, there is a significant degree of uncertainty associated with the vulnerability of the BEB transit systems and their robustness against disruptive events. As such, it is essential to assess the robustness of BEB systems to inform the optimal BEB system configuration.

3. Methodology

3.1. Problem Description

Infrastructure disruption for BEB transit systems can happen due to two main reasons: electricity outages and charging station malfunction. Although there are other types of transit operation disruptions (e.g., congestions, etc.), here we focus on BEB charging infrastructure disruptions. Figure 1 represents a hypothetical example of the charging scheme for two BEBs operating on the same route (inbound and outbound). The BEBs are served by an en-route charging station. A disruption before the scheduled charging event (e.g., an electricity outage in the charging station) will have varying impacts on the operation of this route.

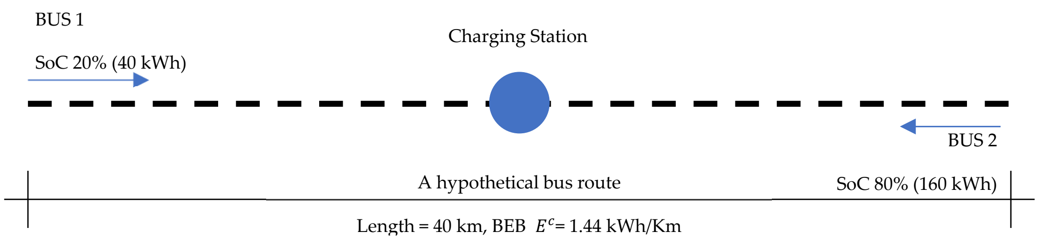

Figure 1. A hypothetical example of the uncertainty in the BEB system's vulnerability.

If the charging station is disrupted (e.g., no power or charger malfunction), BUS 1 will not be able to complete the assigned trip, given that the battery State of Charge (SoC) is lower than the required energy to complete the trip. In comparison, BUS 2 will complete the assigned trip as their SoC is higher, yet the scheduled charging event will be shifted to another time (if available).

Therefore, BEB's infrastructure disruption entails the assessment of the spatiotemporal utilization of the charging network, BEB's SoC, and transit timetables. Given the interdependency of these three elements, several complex scenarios arise during disruption.

First, some BEBs will not be able to complete their assigned trips on the available SoC (immediate operation impact). Second, some BEBs will be able to complete their trips;

however, they will not be able to charge in the rolling horizon (shifted operation impact). Third, the shifted charging/energy demand will be higher than the capacity of the utility grid (cumulative utility impact).

Therefore, assessing BEB transit system disruption should consider the spatiotemporal features of (1) transit operation (timetable and BEB SoC over time), (2) the charging scheme including schedule, location, and utilization time, and (3) the utility grid specification.

To address this issue, we (1) optimized a BEB transit system using the dominant optimization technique in the literature. (2) Extract the resultant BEB system configuration, including battery size, chargers' rated power, spatial allocation, and the charging schedule. (3) Model the BEB transit system as a directed weighted network and subject the network to charging station (node) distribution. (4) Quantify the BEB system robustness by evaluating the cascading impacts on the BEB transit system. (5) Conduct sensitivity analysis to identify how the operational parameters influence the robustness of BEB transit systems. Figure 2 details these procedures.

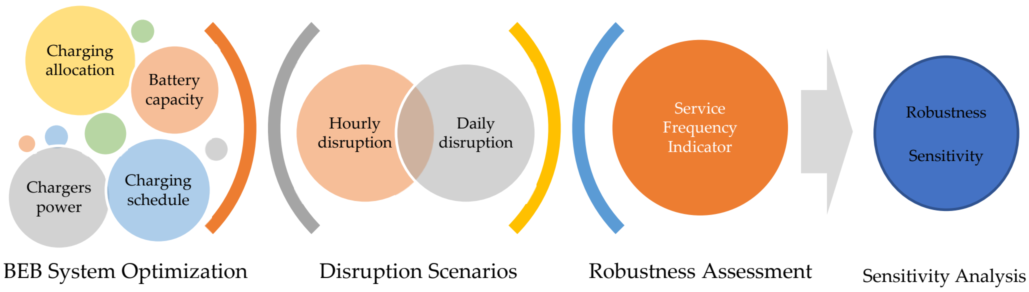

Figure 2. Robustness Assessment Process.

It should be noted that the contribution of the present study is not claimed from the optimization model. The contribution is associated with the measurement of BEB system robustness against charging infrastructure disruption. The optimization model is used as input to feed the network disruption model. Second, the study is not aimed at offering a service rescheduling solution, and we treat the scheduled timetable as a hard constraint in the paper that must be satisfied.

3.2. Optimization Model: Mathematical Formulation

In this work, the optimization model satisfies the objective functions and constraints based on recent BEB literature. Overall, the model minimizes the total system cost by considering infrastructure, fleet, and operation. The model satisfies three common assumptions:

- The charging process is carried out using both en-route charging during the recovery time as well as overnight at the depot;
- The charger-rated powers for all stations are homogenous [6];
- The battery sizes for all buses are homogeneous, enabling flexibility of operation [44];
- The model maintains the current fleet size and the operational timetable [13];
- The model accommodates the electricity time of use (ToU) tariff [24].

In particular, the model identifies the optimal number and locations of the charging stations, which are selected from a set of candidate stations (I). Furthermore, the model quantifies the optimal configuration of each charging station $i \in I$, (i.e., the number of chargers N_i and the rated power P^{ch}). From a fleet perspective, the model chooses the optimal battery capacity for the fleet E^{bat} from a set of battery capacities A^{bat}. A list of abbreviations and notations used in the BEB system optimization model is presented in Table 3.

Table 3. Abbreviations and notations summary.

Abbreviation	Description	Index	Description
GHG	Greenhouse gas	i, i'	Index of candidate charging station location
e-Buses	Electric buses	b	Index of BEBs
ICE	Internal combustion engine	j	Index of sub-trips (the distance between each two consecutive candidate locations)
FCEB	Fuel cell electric bus	t	Index of timeslots
BEB	Battery electric bus	**Variables**	**Description**
ESS	Energy storage system	F_{cons}	Cost of charging stations constructions ($)
SoC	State of charge	$F_{chargers}$	Cost of chargers ($)
TCO	The total cost of ownership	F_{fleet}	Cost of bus fleet, including battery ($)
ToU	Time-of-use	F_{maint}	Cost of maintenance ($)
Sets	**Description**	F_{op}	Cost of electricity ($)
I	Set of candidates charging stations locations	F_{system}	Total annual system cost
B	Set of BEBs	$S^{arr}_{b,j,i}$	Arrival battery energy of bus b after sub-trip j at charging station i (kWh)
J_b	Set of sub-trips of bus b	$S^{dep}_{b,j,i}$	Departure battery energy of bus b before sub-trip j from charging station i (kWh)
A^{ch}	Set of charger-rated powers	$E^{c}_{b,j,i}$	Energy consumption of bus b during sub-trip j after departure from charging station i
A^{bat}	Set of battery-rated energies		
Decision variables	**Description**		
x_i	Binary decision variable, $x_i = 1$ if the location i is selected to build a charging station, $x_i = 0$ otherwise		
N_i	A non $-$ negative integer indicates the number of the chargers deployed in location $i \in I$		
P^{ch}	Charger-rated power (kW)		
E^{bat}	BEBs battery-rated energy for all buses (kWh)		
$y_{b,j,i,t}$	Binary decision variable, $y_{b,j,i,t} = 1$ if the bus b charged at timeslot t in charging station i after sub-trip j, $y_{b,j,i,t} = 0$ otherwise		
$\rho_{b,j,i,t}$	Binary variable, $\rho_{b,j,i,t} = 1$ if the charged state of bus b after sub-trip j in the charging station i for the current timeslot t and the later timeslot t + 1 changes, $\rho_{b,j,i,t} = 0$ otherwise		
$\sigma_{b,j,i,t}$	Binary variable, $\sigma_{b,j,i,t} = 1$ if the charged state of bus b after sub-trip j in the charging station i for the current timeslot t and the previous timeslot $t - 1$ changes, $\sigma_{b,j,i,t} = 0$ otherwise		
Parameters	**Description**	**Parameters**	**Description**
C^{cons}	Cost of construction of candidate charging station i ($)	$e^{f}_{b,j}$	The energy consumption rate of bus b during sub-trip j (kWh/km)
C^{ch}	Charger cost that is related to its power ($/kW)	$e^{bat}_{b,j}$	The energy consumption rate of bus b during sub-trip j caused by one unit of BEB battery size for 1 km distance (1/km)
C^{ch}_{f}	charger fixed cost ($/unit)	r^{m}	Maintenance cost percentage from purchase cost (%)
C^{bat}	Battery cost ($/kWh)	$C_e(t)$	Electricity rate in timeslot t depending on ToU ($/kWh)

Table 3. *Cont.*

C_f^{bus}	Bus cost without battery ($/bus)	θ	Number of workdays
T_s	Timeslot duration (min)	μ_0	Discount rate (%)
$w_{b,j}$	Route factor of bus b in sub-trip j	β	Lifespan (years)
N_i^m	Maximum limit of the number of chargers in charging station i	r^{min}	Minimum limit (%)
$R_{b,j,i}$	Recovery time set of bus b after sub-trip j at charging station i	r^{max}	Maximum limit (%)
η^{ch}	Charger efficiency (%)	$d_{b,j}$	Length of sub-trip j of bus b (km)

The objective function of the model is described in Equation (1). F_{system} denotes the overall BEB system annual cost, which includes charging station construction cost F_{cons}, chargers cost $F_{chargers}$, fleet cost F_{fleet}, maintenance cost F_{maint}, and operation cost F_{op}.

All cost parameters in Equation (1), except the operational cost, are calculated for the system lifespan. Therefore, these parameters are multiplied by an annualized factor related to the lifespan β and the discount rate μ_0 to annualize the cost of the system.

$$F_{system} = \left(F_{cons} + F_{chargers} + F_{fleet} + F_{maint}\right)\left(\frac{\mu_0(1+\mu_0)^{\beta}}{(1+\mu_0)^{\beta} - 1}\right) + F_{op} \tag{1}$$

The five individual costs in Equation (1) are calculated using Equations (2)–(6). The construction cost is estimated in (Equation (2)), Where x_i, $i \in I$ is a binary decision variable that denotes whether a charging station will be installed in location i or not, and I is the set of candidates charging stations. The charger cost is considered in (Equation (3)) as a linear function of the charger-rated power with a constant [2], where N_i is the number of chargers deployed in location i, P^{ch} is the charger's power (kW), C^{ch} is the charger cost related to the charger power ($/kW), and C_f^{ch} is the fixed cost ($).

The fleet cost Is presented in Equation (4) in two parts; the cost of the battery, C^{bat} ($/kWh), which is related to the battery capacity E^{bat} (kWh), and the cost of the bus, C_f^{bus} ($). The maintenance cost is calculated in (Equation (5)) as a percentage, r^m, of the purchase cost of the infrastructure, chargers, and fleet costs. Lastly, the operational cost is the electricity cost, which is related to the ToU tariff $C_e(t)$ ($/kWh), as described in (Equation (6)). Where θ is the number of network workdays, T_s is the timeslot duration (h), P^{ch} is the charger-rated power (kW), and $y_{b,j,i,t}$ is a binary decision variable that denotes whether bus $b \in B$ will charge after sub-trip $j \in J_b$ in location $i \in I$ during timeslot $t \in T$ or not.

$$F_{cons} = \sum_{i \in I} C^{cons} x_i \tag{2}$$

$$F_{chargers} = \sum_{i \in I} N_i (P^{ch} C^{ch} + C_f^{ch}) \tag{3}$$

$$F_{fleet} = \sum_{b \in B} (C^{bat} E^{bat} + C_f^{bus}) \tag{4}$$

$$F_{maint} = r^m \left(F_{con} + F_{chargers} + F_{fleet}\right) \tag{5}$$

$$F_{op} = \theta T_s \left[\sum_{b \in B} \sum_{t \in T} \sum_{i \in I} \sum_{j \in J_b} C_e(t) P^{ch} y_{b,j,i,t}\right] \tag{6}$$

The total annual system cost in (Equation (1)) will be minimized under a set of constraints. First, the battery capacity constraints are presented in Equations (7)–(9). In Equations (7) and (8), the arrival ($S^{arr}_{b,j,i}$)\departure ($S^{dep}_{b,j,i}$) battery energy for the bus b at\from the candidate charging stations i after\before accomplishing the sub-trip j ($S^{arr}_{b,j,i}$) should be greater\less than a minimum\maximum threshold ratio ($r^{min}\backslash r^{max}$) from the battery size E^{bat}. These constraints are applied to all buses, $b \in B$, and for all sub-trips, $j \in J_b$, except for the departure for the first sub-trip. The battery capacity equals the maximum threshold as presented in (Equation (9)).

$$S^{arr}_{b,j,i} \geq r^{min} E^{bat} \quad \forall b \in B, \forall j \in J_b, i \in I \tag{7}$$

$$S^{dep}_{b,j,i} \leq r^{max} E^{bat} \quad \forall b \in B, \forall j \in J_b, i \in I \tag{8}$$

$$S^{dep}_{b,1} = r^{max} E^{bat} \quad \forall b \in B \tag{9}$$

Equation (10) dictates that the arrival battery capacity for any bus b from a sub-trip j in location i' is equal to the departure battery energy from the previous location i mines the energy consumed during the sup-trip j from i to i' ($E^c_{b,j,i}$). The energy consumption rate for each sub-trip is taken as a linear function of the battery capacity. The energy consumption for each sub-trip is calculated by multiplying the driving distance $d_{b,j}$ of the sub-trip j by the energy consumption rate ($e^f_{b,j} + e^{bat}_{b,j} E^{bat}$) and the sub-trip route factor $w_{b,j}$ which is related to the road and traffic conditions following [5].

$$S^{arr}_{b,j,i'} = S^{dep}_{b,j,i} - E^c_{b,j,i} \quad \forall b \in B, \forall j \in J_b, i\&i' \in I \tag{10}$$

$$E^c_{b,j,i} = d_{b,j}\left(e^f_{b,j} + e^{bat}_{b,j} E^{bat}\right) w_{b,j} \quad \forall b \in B, \forall j \in J_b, i \in I \tag{11}$$

The charging strategy constraints in Equations (12)–(16) state that the departure battery energy $S^{dep}_{b,j+1,i}$ of bus b from location i for sub-trip $j+1$ is equal to the summation of the arrival energy $S^{arr}_{b,j,i}$ from the previous sub-trip j and the charged energy during the recovery time $R_{b,j,i}$, if it exists. The charged energy during the recovery time is related to the charger-rated power P^{ch}, charger efficiency η^{ch}, and the decision if the bus was charged or not $y_{b,j,i,t}$. The charger decision of bus b after sub-trip j in location i during the timeslot t ($y_{b,j,i,t}$) is set to zero during the operation time $\forall t \notin R_{b,j,i}$, as mentioned in (Equation (13)). As the time is discretized, Constraints (14)–(16) are used to ensure the charging continuity of each charging event. These constraints are drawn from the work of [45]. While $\rho_{b,j,i,t}$ and $\sigma_{b,j,i,t}$ are auxiliary variables used to calculate the change of the charging state during the recovery time. In addition, Constraint (16) emphasizes that if the bus charges, the change from the state of not charging to charging is only one and the same for the change from charging to not charging to ensure the charging continuity.

$$S^{dep}_{b,j+1,i} = S^{arr}_{b,j,i} + \sum_{t \in R_{b,j,i}} \eta^{ch} T_s P^{ch} y_{b,j,i,t} \quad \forall b \in B, \forall j \in J_b, i \in I \tag{12}$$

$$y_{b,j,i,t} = 0 \quad \forall b \in B, \forall j \in J_b, i \in I, \forall t \notin R_{b,j,i} \tag{13}$$

$$\rho_{b,j,i,t} \geq y_{b,j,i,t} - y_{b,j,i,t+1} \quad \forall b \in B, \forall j \in J_b, i \in I, \forall t \in R_{b,j,i} \tag{14}$$

$$\sigma_{b,j,i,t} \geq y_{b,j,i,t} - y_{b,j,i,t-1} \quad \forall b \in B, \forall j \in J_b, i \in I, \forall t \in R_{b,j,i} \tag{15}$$

$$\sum_{t \in R_{b,j,i}} \rho_{b,j,i,t} = \sum_{t \in R_{b,j,i}} \sigma_{b,j,i,t} \leq 1 \quad \forall b \in B, \forall j \in J_b, i \in I, \forall t \in R_{b,j,i} \tag{16}$$

For the charging station constraints, (Equation (17)) ensures no charger deployment in location i without selecting the location as a charging station. In addition, it constrains the number of chargers deployed in location i by an upper limit N^m_i which is related to the available area in site i. In Equation (18), the number of buses charged in location i should be lower than the number of chargers available.

$$N_i \leq N_i^m x_i \quad \forall i \in I \tag{17}$$

$$\sum_{b \in B} y_{b,j,i,t} \leq N_i \quad \forall i \in I, \forall t \in T \tag{18}$$

For the variable's types of constraints, Equations (19)–(25) emphasize that x_i, $y_{b,j,i,t}$, $\rho_{b,j,i,t}$, and $\sigma_{b,j,i,t}$ are binary, N_i is a non-negative integer, and P^{ch} and E^{bat} are selected from predefined sets containing different finite predefined levels.

$$x_i \in \{0,1\} \quad \forall i \in I \tag{19}$$

$$N_i \in Z^{0+} \quad \forall i \in I \tag{20}$$

$$P^{ch} \in A^{ch} \tag{21}$$

$$E^{bat} \in A^{bat} \tag{22}$$

$$y_{b,j,i,t} \in \{0,1\} \quad \forall b \in B, \forall j \in J_b, i \in I, \forall t \in R_{b,j,i} \tag{23}$$

$$\rho_{b,j,i,t} \in \{0,1\} \quad \forall b \in B, \forall j \in J_b, i \in I, \forall t \in R_{b,j,i} \tag{24}$$

$$\sigma_{b,j,i,t} \in \{0,1\} \quad \forall b \in B, \forall j \in J_b, i \in I, \forall t \in R_{b,j,i} \tag{25}$$

The utilized optimization model for the BEB system design is formulated as follows:

$$Min\ (1)$$

$$s.t.\ (7-25)$$

The optimization model in this formulation is represented as an integer non-linear programming. The non-linearity exists in Equations (3), (6) and (12). The charger-rated power (P^{ch}) is the common variable in all the non-linear terms. In addition, the model considers the homogeneity feature of the charger-rated power for the entire network (P^{ch}). Therefore, the utilized optimization model could be linearized using a scenario-based optimization approach by solving the model several times using each level of the charger-rated power in A^{ch} set (finite set), compare them and select the one that minimizes the objective function. In this case, the linear model will be solved $\left|A^{ch}\right|$ times, and it will be converted to an integer linear programming (ILP) model.

Several methods and algorithms have been developed to solve ILP models [46]. Branch and bound, cutting plane algorithm, dynamic programming, linear programming relaxation methods (e.g., Lagrangian relaxation), metaheuristics, and population-based evolutionary algorithms [47]. These methods can be used alone or in combination to solve ILP problems such as branch and price, branch and cut, and decomposition methods (e.g., Benders' decomposition and column generation technique) [48]. A detailed description of each method can be found in [47].

Any commercial solver developed for these methods could handle the ILP model in a reasonable computational time (e.g., Gurobi and CPLEX). As such, and based on the formulation of the proposed model, the model is solved using the Gurobi solver.

3.3. Complex Network Representation for BEB Transit System

The BEB transit system consists of e-buses operating several tips that connect between stops/stations on predefined routes, as shown in Figure 3a. The BEB transit system is represented through a Complex Network approach. As such, the system is modeled as a directed weighted network that consists of nodes and links, as shown in Figure 3b.

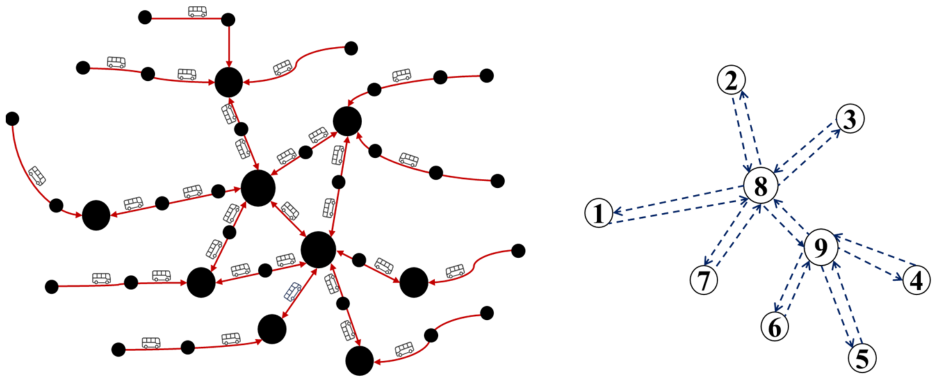

(**a**) (**b**)

Figure 3. A hypothetical example of the BEB representation in complex network theory. (**a**) BEB transit system; (**b**) BEB in complex network theory. Black dots represent bus stops/stations in the network; red lines represent bus routes; white circles represent the charging stations (nodes); dashed blue lines represent the directed bus trips (links).

The charging stations (output of the optimization) represent *nodes*. In comparison, *links* are represented by the number of BEBs connected to each charging station. Using this classification, the Degree Centrality measure (C_D) in Equation (26) [49] represents the total number of bus links connected to each charging station in the network (undirected network), which is divided into in-degree (Equation (27)) and out-degree (Equation (28)) (directed network). Where, $\overleftarrow{a}_{ij}$ and $\overleftarrow{a}_{ji}$ are the number of buses going to and from j, respectively. The total number of buses operating on a link between i and j is $a_{ij} = \overleftarrow{a}_{ij} + \overleftarrow{a}_{ji}$. J' is the set of stations connected to j.

$$\text{Degree Centrality } C_D \quad C_D(j) = \sum_{i=1}^{J'} a_{ij} \tag{26}$$

$$\text{In} - \text{Degree Centrality } \left(C_D^{in}\right) \quad C_D^{in}(j) = \sum_{j=1}^{J'} \overleftarrow{a}_{ij} \tag{27}$$

$$\text{Out} - \text{Degree Centrality } \left(C_D^{out}\right) \quad C_D^{out}(j) = \sum_{j=1}^{J'} \overleftarrow{a}_{ji} \tag{28}$$

The robustness of the BEB system is evaluated under charging infrastructure disruption using the service frequency indicator R_t^{freq} in Equation (29). It estimates, during the duration of the disruption, the losses in transit trips due to the disruption. In other words, BEBs that will not be able to charge during disruption and their SoC cannot satisfy the next trip will be deemed unavailable, and their assigned trips will be canceled.

Numerically, it represents the ratio between the frequency of bus trips (for each time $t \in T$) operating on the network after disruption (N_t^D) to the total daily frequency (N^{Total}).

$$R_t^{freq} = \frac{N_t^D}{N^{Total}} \times 100 \quad \forall\, t \in T \tag{29}$$

It should be noted that: (1) BEBs are removed from operation if the available battery SoC is insufficient to complete their trips during the disruption time. In case SoC values are sufficient, no BEBs are removed from the network. (2) We did not re-distribute BEBs to other charging stations outside their routes, as the reallocation will also result in canceling the assigned trips.

Furthermore, two disruption scenarios are considered for the charging stations (nodes). First, we assume a node disruption that will be resolved within the next hour. This is referred to as **hourly disruption**. In this scenario, each charging station is disrupted for one hour, and the impacts of this disruption are assessed for each charging station. Second, we assume a node disruption that will be resolved by the end of the operation day. This is referred to as **daily disruption**. During the daily disruption, the charging station is assumed to be out of service from the disruption time till the next day of operation. In this case, the impact of the daily disruption during each operation hour is also assessed for each charging station independently. For each scenario, the two robustness indicators are quantified, and the impact of each charging station on the system's robustness is assessed.

A methodological flowchart summarizing the methods used in this research is shown in Figure 4.

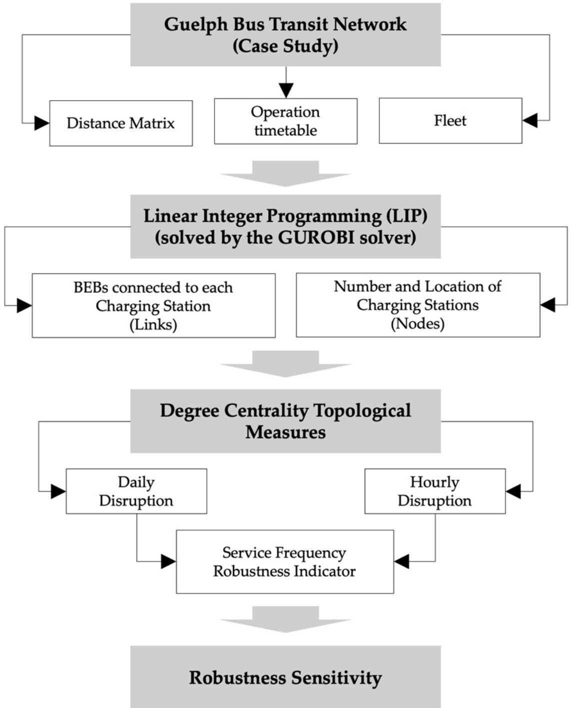

Figure 4. Methodological flowchart.

4. Case Study

The Guelph bus transit network is selected as the case study. Located in Guelph City, Ontario, Canada, this medium-size multi-hubs network operates a fleet of 55 buses that travel 5,144,238 km (478,120 trips) annually while transporting around 110,000 passengers daily.

The network dataset is collected for weekday operation from the REMIX platform [50] and timetable data [51]. Both are based on the general transit feed specification (GTFS) data of Guelph. A brief description of Guelph's operation data is illustrated in Table 4.

Guelph network consists of 23 bus routes operating through 506 bus stops/stations (see Figure 5a). Using the longitude and latitude data for each bus stop/station, we estimated the distances between each pair of stops/stations; then, we estimated the consumed energy for each bus trip using the calibrated model [5,9]. Stations that serve more than one route (e.g., transfer and end stations) are identified as candidate locations for charging stations "*candidate charging stations*". This follows previous research, such as the work of [12,16,37,52]. As a result, we obtained 19 candidate locations for charging stations, as shown in Figure 5b.

Table 4. Timetable data for each bus route in the Guelph bus transit network.

Route ID	T_r^{start}	T_r^{end}	T_r^{trip} (min) *	Av. Headway Time (min)	l(r) (km)	Ntrips,r (#)
1A-College Edinburgh	5:45	24:15	14	30	18.016	76
2A-West Loop Clockwise	5:45	24:15	26	30	35.354	76
3A-East Loop Clockwise	6:00	22:30	43	13	24.528	148
1B- College Edinburgh	5:45	24:15	15	30	18.910	76
3B-East Loop	5:45	24:15	24	30	35.856	64
4-York	5:45	24:15	26	30	10.453	38
5-South Gordon	5:45	24:15	55	30	30.124	76
6-Harvard Ironwood	5:45	24:15	26	30	14.589	76
7-Kortright Downe	5:45	24:15	26	30	19.065	76
8-Stone Road Mall	5:45	24:15	26	30	9.504	38
9-West End Community Centre	5:45	24:15	26	30	11.189	38
10-Imperia	5:45	24:15	28	30	10.500	38
11-Willow West	5:45	24:15	28	30	10.130	38
12-General Hospital	5:45	24:15	26	30	10.289	38
14-Grange	5:45	24:15	25	30	9.755	38
15-College Ave W	5:45	24:15	26	30	13.951	76
16-Route 16	5:45	24:15	54	30	32.117	76
20-Northwest Industrial	5:45	24:15	51	30	29.748	76
50-Route 50	8:00	21:40	13	20	5.178	42
56-Route 56	7:45	21:45	7	30	11.440	58
57-Route 57	7:45	22:25	15	20	8.305	90
58-Route 58	7:45	21:50	15	45	8.523	82
Gordon Corridor	7:45	19:00	24	36	14.913	36

* The data represent inbound and outbound trips. For each route (r): T_r^{start} is the beginning of the operation time; T_r^{end} is the end of the operation time; T_r^{trip} is the time duration for each bus trip; $l_{(r)}$ is the total distance, and $N_{trips,r}$ is the total number of daily trips for route *r*.

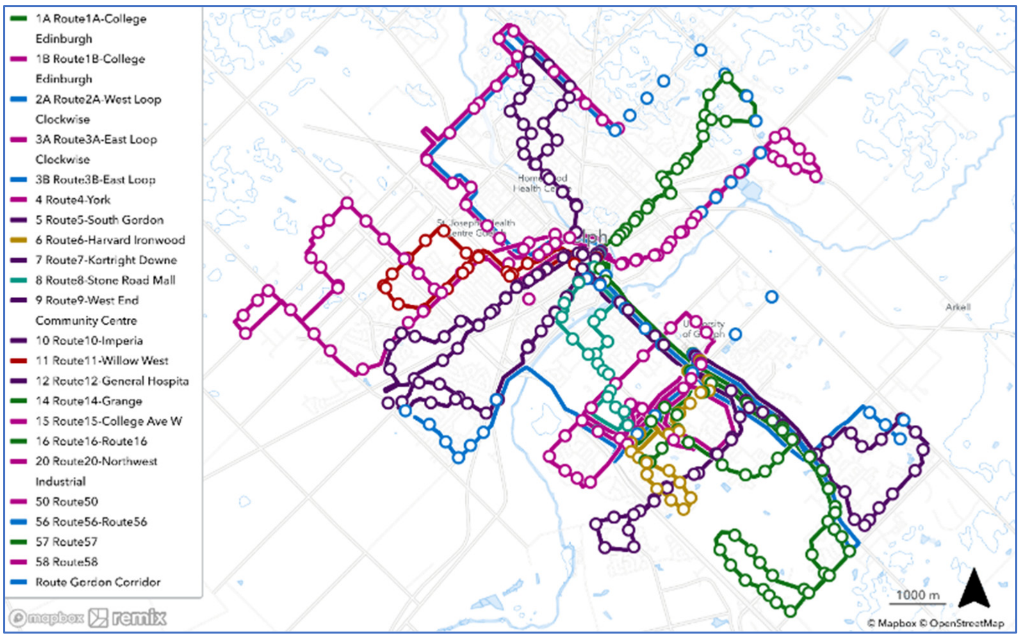

(**a**)

Figure 5. *Cont.*

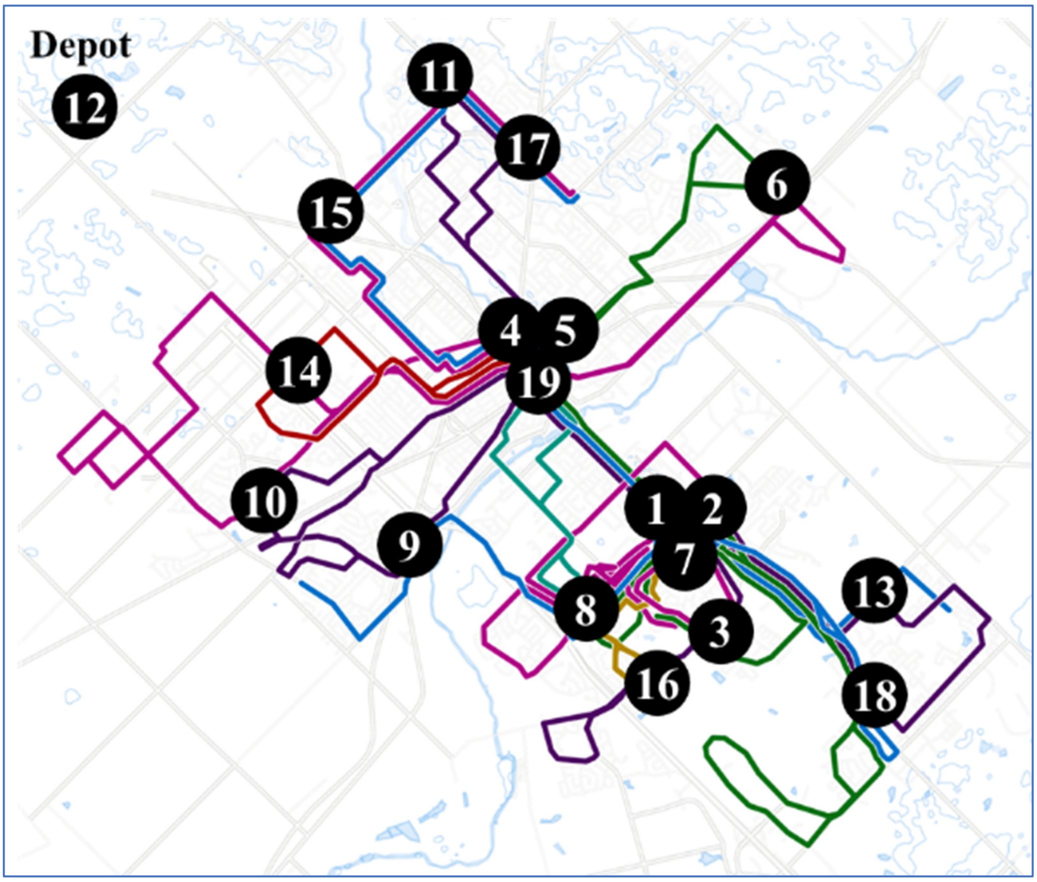

(**b**)

Figure 5. The distribution of bus stops/stations and candidate charging stations in the Guelph bus network. (**a**) Bus stops/stations in the network (n = 506); (**b**) Candidate charging stations (n = 19).

5. Results

5.1. Optimal BEB System Configuration

The model is coded in MATLAB and solved using the GUROBI solver. The model runs on a personal computer with Intel® Core i5, 16 GB Ram, and a 4.20 GHz CPU. Overall, there are 67,011 variables and 82,703 constraints in the study. The optimal solution was reached in 4 min and 26.17 s.

The results indicate that BEBs could be implemented for Guelph transit. The system configuration includes 55 BEBs, each with a battery of 100 kWh (homogonous BEB fleet), with a total energy demand of 28,853.33 kWh/day. In addition, out of the 19 candidate charging stations, seven charging stations are required for the system with varying rated power and number of chargers (Table 5). The total annual system cost is $4,840,277.81, distributed as detailed in Figure 6.

The optimization model allocated seven charging stations out of the 19 candidate stations (Table 5). Charging station #1 includes two chargers, and charging station #4 contains four chargers. Therefore, the total number of chargers in the network is 11 chargers. The spatial distribution of the charging stations is depicted in Figure 7. Given that a homogonous charger power is assumed, all chargers have a rated power of 400 kW.

In particular, Table 5 details the locations of the charging stations, the number of chargers at each station, and the routes served by each charging station. It is observable from the data that Charging station #12, located at the depot, is shared between all the buses; hence it serves all routes at night. In comparison, Charging stations #13 and #15 serve fewer bus routes.

Table 5. Configuration of the charging stations and the corresponding bus routes.

Charging Station ID	Station Name	Number of Chargers per Station (#)	Bus Routes
1	UC South Loop	2 (1-1, 1-2)	1A, 1B, 5, 6, 7, 15, 57
4	GCS East	4 (4-1, 4-2, 4-3, 4-4)	2A, 3B, 4, 5, 8, 9, 10, 11, 12, 14, 16, 20
7	Gordon St. at Harvard Rd.	1	3A, 6, 7
12	Depot	1	1A, 1B, 2A, 3A, 3B, 4, 5, 6, 7, 8, 9, 10, 11, 12, 14, 15, 16, 20, 50, 56, 57, 58, GC
13	Goodwin Dr. at Ray Cres.	1	2A, 5
15	Woodlawn at Wal-Mart	1	3B
19	University	1	50, 56, 57, 58, GC

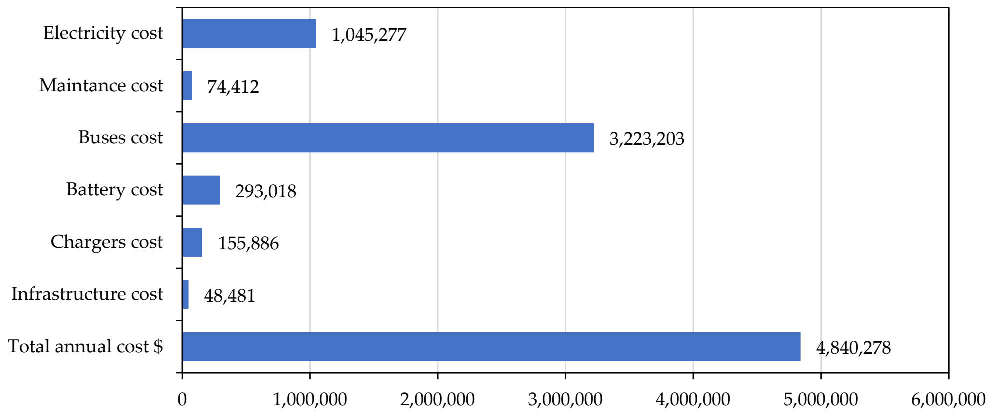

Figure 6. The total annual costs of implementing the BEB system in Guelph city.

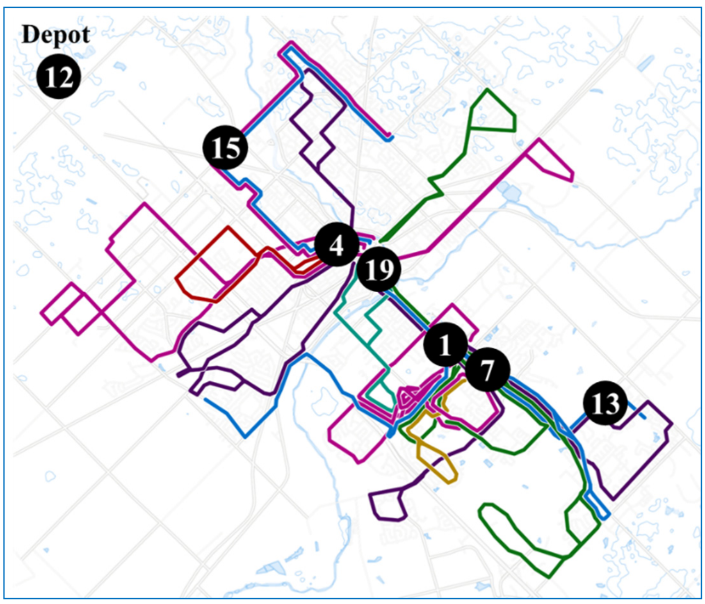

Figure 7. Charging stations' locations with ID.

Collectively, the BEB fleet utilizes the charging infrastructure for 2656 min (Table 6—the sum of column 4), and the maximum charging duration for a bus is 37 min/hour. While the total number of charging events is 1104 events/day (Table 6—the sum of column 7), and the maximum number of hourly charging events per charger is seven events/hour (Table 6—column 9).

Table 6. The hourly charging utilization.

Hour	Number of Utilized Charging Stations (#)	Charging Stations IDs	Charging Duration (Minute)			Number of Charging Events (#)			Number of Buses at Each Charging Station (#)
			Sum.	Min.	Max.	Sum.	Min.	Max.	
(1)	(2)	(3)	(4)	(5)	(6)	(7)	(8)	(9)	(10)
5:00 AM	1	12	44	44	44	7	1	1	7
6:00 AM	6	1, 4, 7, 12, 13, 15	180	8	34	57	1	6	40
7:00 AM	5	1, 4, 7, 13, 15	130	4	26	38	1	5	32
8:00 AM	6	1, 4, 7, 13, 15, 19	176	6	34	51	1	6	37
9:00 AM	6	1, 4, 7, 13, 15, 19	160	2	38	46	1	6	36
10:00 AM	6	1, 4, 7, 13, 15, 19	164	6	32	51	1	6	36
11:00 AM	6	1, 4, 7, 13, 15, 19	292	12	42	68	1	6	44
12:00 PM	6	1, 4, 7, 13, 15, 19	256	6	38	61	1	6	44
1:00 PM	6	1, 4, 7, 13, 15, 19	228	12	40	57	1	7	40
2:00 PM	6	1, 4, 7, 13, 15, 19	258	12	42	59	1	6	42
3:00 PM	6	1, 4, 7, 13, 15, 19	260	12	46	67	1	6	45
4:00 PM	6	1, 4, 7, 13, 15, 19	284	12	42	75	1	6	46
5:00 PM	5	1, 4, 7, 13, 15	118	2	28	32	1	5	26
6:00 PM	5	1, 4, 7, 13, 15	120	2	24	37	1	6	28
7:00 PM	7	1, 4, 7, 12, 13, 15, 19	270	12	40	75	1	7	46
8:00 PM	7	1, 4, 7, 12, 13, 15, 19	296	12	40	71	2	7	45
9:00 PM	7	1, 4, 7, 12, 13, 15, 19	276	12	46	65	1	6	43
10:00 PM	7	1, 4, 7, 12, 13, 15, 19	220	10	44	58	1	6	36
11:00 PM	6	1, 4, 7, 12, 13, 15	210	12	42	47	1	6	36
12:00 AM	6	1, 4, 7, 12, 13, 15	202	8	42	51	1	6	34
1:00 AM	3	1, 4, 12	66	2	44	13	1	3	11
2:00 AM	1	12	36	36	36	6	1	2	6
3:00 AM	1	12	28	28	28	6	1	2	6
4:00 AM	1	12	46	46	46	6	1	1	6

The seven charging stations satisfy the charging demands of 23 bus routes (55 buses). We listed the hourly charging flow for each operation hour in Table 6. The results also indicate a significant variation in the utilization rates of the charging stations. This is attributed to the varying spatiotemporal energy demand induced by the transit operation timetable and the varied BEB energy consumption. The two energy demand peaks could be observed (shaded cells in Table 6) from 11:00 AM to 4:00 PM and from 7:00 PM to 9:00 PM.

Furthermore, the charging utilization rates (number of charging events) per route are depicted in Table 7. As seen in the last column, the number of charging events varies significantly per route. This is attributed to the route features, including length, headway, and energy consumption.

Table 7. Hourly chagrining events per route.

Route Name	1A	1B	2A	3A	3B	4	5	6	7	8	9	10	11	12	14	15	16	20	50	56	57	58	GC	Total
Fleet Size	3	2	4	11	3	1	4	2	2	1	1	2	1	1	1	1	3	3	1	2	2	2	2	55
5:00 AM	0	0	1	1	0	0	1	0	0	0	1	1	1	0	0	0	1	0	0	0	0	0	0	7
6:00 AM	3	4	3	3	5	2	5	4	6	2	2	2	2	2	2	1	3	3	0	0	1	1	1	57
7:00 AM	2	2	3	5	4	1	5	1	3	1	1	0	1	1	2	0	4	2	0	0	0	0	0	38
8:00 AM	2	2	4	4	5	2	5	4	6	1	1	1	1	1	1	0	4	3	0	0	0	2	2	51
9:00 AM	2	1	4	5	6	1	6	2	4	2	1	1	1	1	1	2	2	3	1	0	0	0	0	46
10:00 AM	2	3	4	4	5	2	6	2	4	2	2	0	2	2	1	1	4	2	0	0	0	2	1	51
11:00 AM	2	3	4	4	5	1	6	3	5	1	2	3	2	2	2	3	4	2	3	2	3	5	1	68
12:00 PM	2	4	4	4	4	2	6	2	4	2	2	1	2	2	1	2	4	3	1	2	4	2	1	61
1:00 PM	2	3	4	4	6	2	7	2	3	2	1	1	2	1	2	3	4	2	1	1	1	2	1	57
2:00 PM	2	3	4	4	6	2	5	3	4	2	2	1	2	1	2	1	4	2	1	2	1	3	2	59
3:00 PM	2	2	4	5	6	1	6	5	6	1	2	2	2	2	2	1	4	2	2	1	2	5	2	67
4:00 PM	1	4	4	6	6	2	6	4	6	2	1	1	2	2	2	5	4	3	2	2	4	2	4	75
5:00 PM	0	2	4	5	5	0	3	0	5	0	1	0	1	0	0	0	3	3	0	0	0	0	0	32
6:00 PM	2	1	4	3	6	2	2	1	4	1	2	0	0	1	1	0	4	2	0	0	0	0	1	37
7:00 PM	3	3	4	4	6	2	7	4	7	2	2	3	2	1	2	2	4	3	1	2	5	4	2	75
8:00 PM	2	4	4	7	6	2	6	3	4	2	2	2	2	2	2	3	4	3	3	2	2	4	0	71
9:00 PM	2	4	4	4	6	1	5	2	4	2	2	2	2	1	2	2	4	3	1	3	4	5	0	65
10:00 PM	2	4	4	2	6	2	6	4	5	1	2	0	2	2	2	2	4	2	0	1	3	2	0	58
11:00 PM	2	2	3	3	6	2	5	3	3	2	1	2	2	1	1	2	3	2	1	1	0	0	0	47
12:00 AM	2	3	4	2	5	2	6	4	5	1	2	2	1	1	1	3	5	2	0	0	0	0	0	51
1:00 AM	0	1	2	0	2	0	3	0	0	1	0	0	0	0	0	1	2	0	0	0	1	0	0	13
2:00 AM	0	0	0	0	1	0	1	1	1	0	0	0	0	0	0	0	0	2	0	0	0	0	0	6
3:00 AM	0	0	2	0	0	0	0	1	1	0	0	1	0	0	0	0	0	1	0	0	0	0	0	6
4:00 AM	1	1	1	0	0	1	0	0	0	0	0	0	1	1	0	0	0	0	0	0	0	0	0	6
Total	38	56	79	79	107	32	108	55	90	30	32	26	33	27	29	34	75	50	17	19	31	39	18	1104

Values in the color-coded cells represent the number of hourly charging events for each route, and the last column and row represent the total.

Along the same lines, the utilization rate (time of use) per charging station varies significantly, as depicted in Table 8. The number of buses operating at each hour and the BEBs' energy demand overtime for each charging station is shown in Appendix A.

Table 8. Hourly chagrining duration (minutes) per charger.

Charger ID	1-1	1-2	4-1	4-2	4-3	4-4	7	12	13	15	19	Total
5:00 AM	0	0	0	0	0	0	0	44	0	0	0	44
6:00 AM	28	20	30	16	10	8	16	34	8	10	0	180
7:00 AM	22	4	24	12	10	10	26	0	12	10	0	130
8:00 AM	24	16	34	18	14	6	30	0	14	12	8	176
9:00 AM	24	8	38	18	8	10	20	0	20	12	2	160
10:00 AM	32	8	22	16	18	16	22	0	16	8	6	164
11:00 AM	42	36	42	28	18	20	40	0	22	12	32	292
12:00 PM	36	22	34	18	18	20	36	0	28	6	38	256
1:00 PM	40	16	32	14	16	22	40	0	22	12	14	228
2:00 PM	42	12	36	28	18	16	42	0	28	12	24	258
3:00 PM	36	16	36	22	18	16	36	0	22	12	46	260

Table 8. *Cont.*

Charger ID	1-1	1-2	4-1	4-2	4-3	4-4	7	12	13	15	19	Total
4:00 PM	42	34	30	26	18	18	40	0	28	12	36	284
5:00 PM	12	2	28	16	14	0	28	0	6	12	0	118
6:00 PM	24	0	24	16	10	4	18	0	14	8	2	120
7:00 PM	40	28	40	22	16	22	20	22	22	12	26	270
8:00 PM	40	24	38	16	26	18	38	28	26	12	30	296
9:00 PM	38	20	46	16	18	16	30	24	22	12	34	276
10:00 PM	44	18	24	14	16	18	28	10	26	12	10	220
11:00 PM	28	12	42	16	16	12	20	34	18	12	0	210
12:00 AM	36	18	24	22	14	14	8	42	12	12	0	202
1:00 AM	2	0	10	6	4	0	0	44	0	0	0	66
2:00 AM	0	0	0	0	0	0	0	36	0	0	0	36
3:00 AM	0	0	0	0	0	0	0	28	0	0	0	28
4:00 AM	0	0	0	0	0	0	0	46	0	0	0	46
Total	632	314	634	360	300	266	538	392	366	210	308	4320

Values in the color-coded cells represent the duration (min) of charging events at each charger, and the last column and row represent the total.

5.2. BEB System Robustness

The results of the service frequency robustness indicator (R_t^{freq}) due to the hourly and daily disruption scenarios reported in Figures 8 and 9, and the numerical results are available in Appendix B. Each line in the graphs should be interpreted as the impact of the disruption to a charging station on the entire network. Please note that the operation ends at 1:00 AM; however, Charging Station # 12 (Depot) operates overnight. Hence the x-axis is fixed to 24 h.

The hourly disruption results (Figure 8) show a relatively small fluctuation in the service frequency robustness indicator associated with the disruption of each charging station. The trend is almost similar over time. In other words, an hourly disruption to any charging station would have the same impact on the service. The service is likely to operate at 97–100% of its original frequency, indicating a robust operation.

In comparison, for multi-charger stations (i.e., charging stations #1 and #4), the results show that the impact of an hourly electricity outage (disruption to all chargers) is significant compared to equipment malfunction (disruption to single chargers). However, the magnitude of impact is still marginal, with robustness values between 97.9% and 97.1% for chargers #1 and #4, respectively.

A daily disruption (Figure 9) to any charging station will reduce the frequency of the service significantly (up to 57%). Like the hourly disruption, multi-charger stations severely impact the service in the case of an electricity outage. It should be noted that each dot in Figure 9 represents the daily impact on the service frequency due to the disruption to the charger at the given time. It also assumes that the disruption will last until the end of the operation day. In other words, each dot is one disruption scenario.

5.3. Sensitivity of BEB Robustness: A Discussion

A Sensitivity Analysis is performed to ascertain how the hourly frequency robustness of the BEB transit system is affected by the BEB charging schedule parameters. These parameters include (a) the number of BEBs charging at each charging station during each hour; (b) the number of charging events during each hour per station; (c) the charging duration, which represents the time that each BEB requires to charge its batteries at each hour; and (d) energy demand represents the total energy demanded at each charging station during each hour.

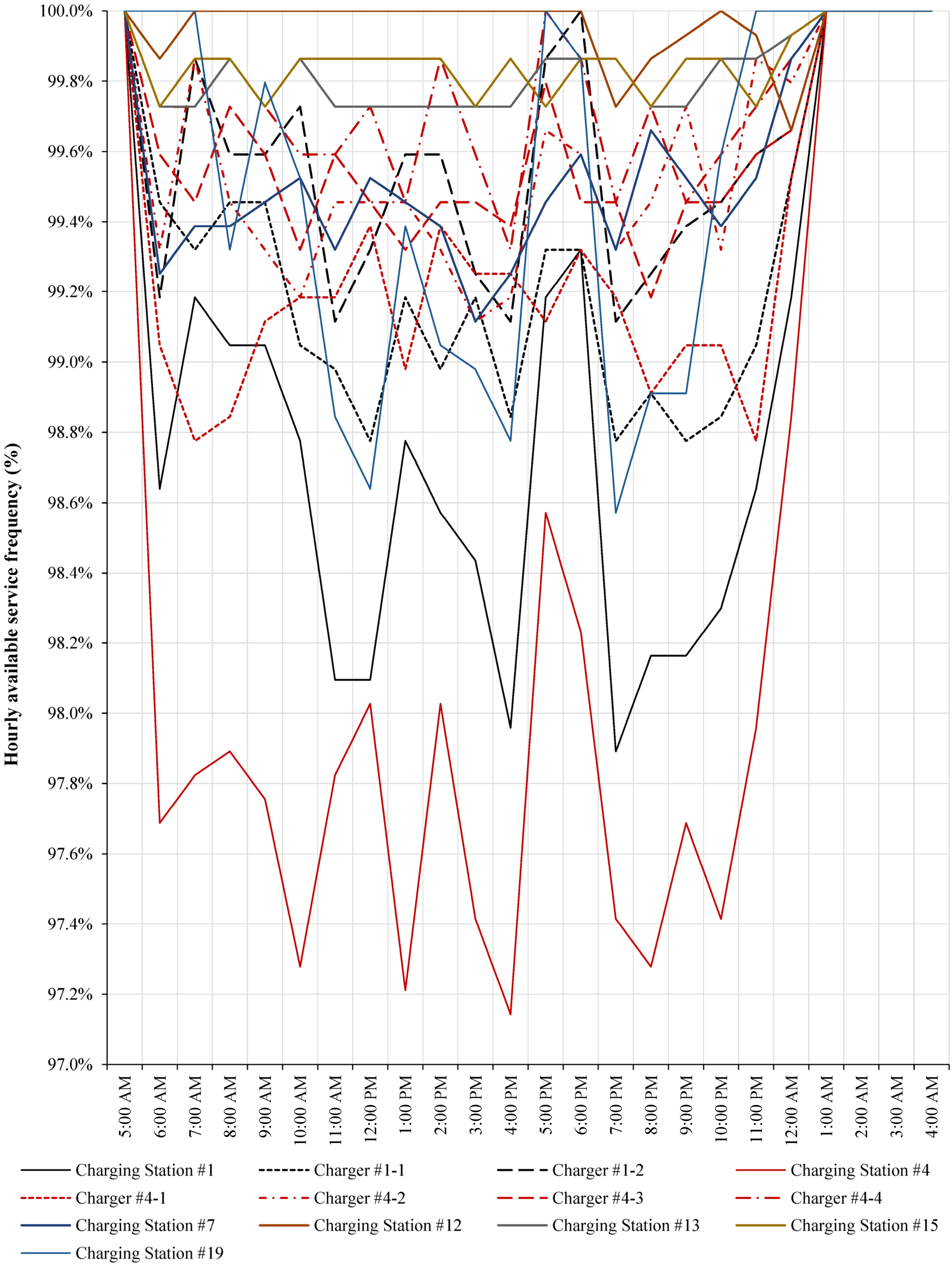

Figure 8. Service frequency reduction due to hourly disruption to each charging station.

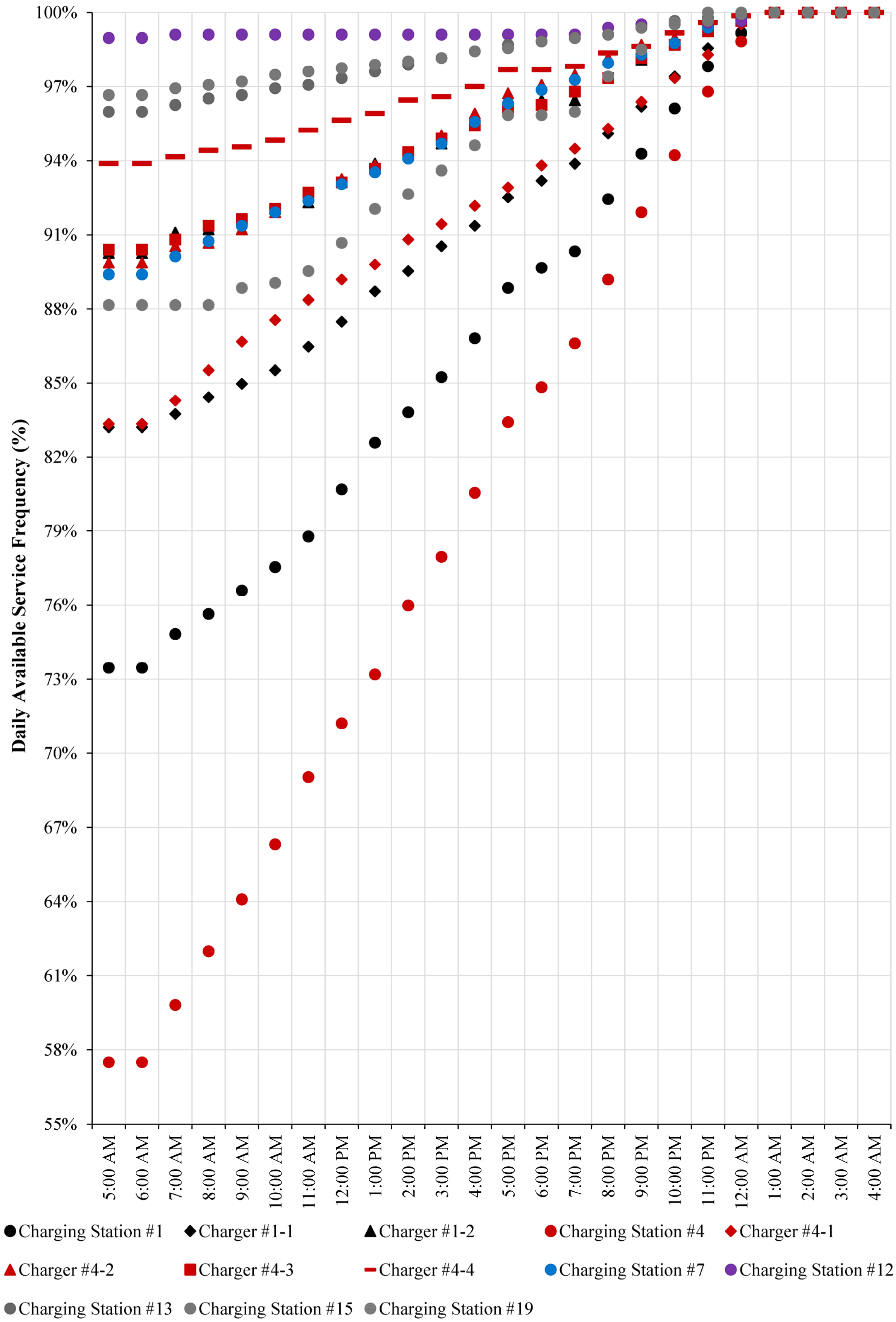

Figure 9. Service frequency percentage due to daily disruption to each charging station.

This study uses a global variance-based sensitivity analysis method, Sobol Indices [53]. Sobol Indices consider the entire input domain and provide a means of gauging the interactions between the parameters. It calculates the robustness variance and decomposes it into input parameter contributions. Two Sobol indices are studied: the first-order effect index S_i, which represents the effect of X_i alone, and the total-order effect index S_{Ti}, considers the interactions of X_i with other parameters as follows:

$$S_i = \frac{V\left[E\left(\frac{Y}{X_i}\right)\right]}{V(Y)} \tag{30}$$

$$S_{Ti} = 1 - \frac{V[E(Y/X_{\sim i})]}{V(Y)} \tag{31}$$

where $V[.]$ and $E(.)$ are the variance and expected values, respectively. The Sobol sampling [54] and Saltelli estimator [55] are utilized to estimate these two indices (Figure 10).

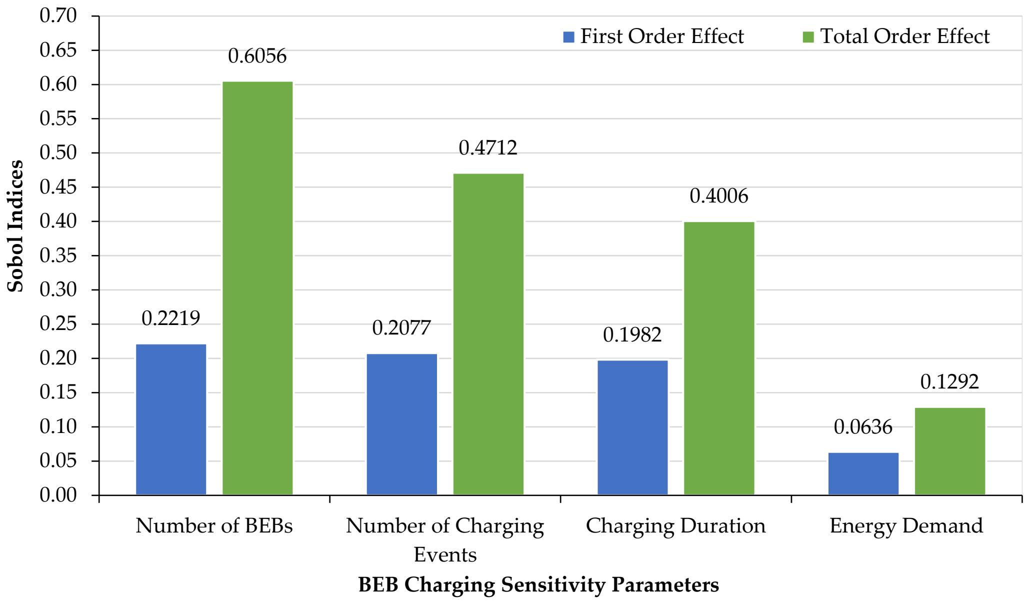

Figure 10. Sensitivity analysis results (first- and total-order effects).

The sensitivity results (Figure 10) show that the number of BEBs charging at each station has the greatest impact on the robustness of the BEB transit system for both first-order and total effects. The number of charging events and their duration have the second and third highest impacts on the BEB system hourly frequency robustness, respectively. In contrast, the energy demand has the lowest influence on robustness.

These results indicate that: First, the charger's power is less impactful, from a service robustness perspective, compared to the number of charging events. In other words, optimizing the charging process to reduce the number of charging events is critical. Second, allocating multiple chargers at the same location severely impacts service robustness. We recommend spatially spreading the charging infrastructure to distribute the risk of having multiple chargers at the same location. This is critical to the depot charging concept.

6. Conclusions

Current BEB infrastructure optimization models adopted in the literature rely on a minimization function of the total system cost, utility impact, and component sizing. However, a minimization function is not optimal for BEB system configuration, particularly when challenged with disruptive events. Furthermore, the cascading impacts of disruptions on the BEB network are still unidentified [28]. As such, there is a clear gap in understanding and assessing the behavior of the BEB transit system during disruption.

This paper answers two primary research questions: First, what is the robustness of the BEB transit system during disruptive events such as electricity outages or equipment malfunction? Second, which charging process parameters significantly affect the robustness of the BEB transit system?

To address these questions, we developed a BEB system configurations optimization model applied to a Guelph bus transit network as a case study. The resultant BEB system configuration is extracted, including the battery size, chargers' spatial distribution, chargers' power, and charging schedule. The extracted results are used as input in a complex network, modeled as a directed weighted graph. The resultant charging stations are subjected to disruptive events representing hourly and daily (discrete events) electricity outages and/or equipment malfunction. The cascading impacts on the BEB transit system are evaluated to quantify the robustness of the bus transit network through a service frequency indicator. Furthermore, the sensitivity of the BEB transit system robustness towards the charging schedule parameters is analyzed.

The results show that the hourly disruption slightly impacts the BEB service frequency robustness. Still, the service can operate with more than 97% of its original frequency, which indicates a robust operation. In contrast, the daily disruption will diminish the service frequency by up to 57% of the total service frequency.

The sensitivity results show that the charging schedule has a noticeable impact on the robustness of the BEB system. The number of charging events and their duration significantly affect the BEB system's robustness. Therefore, reducing the number of charging events is critical to attaining a robust operation. Besides, the multiple chargers assigned to a single location have a deleterious effect on the robustness of the BEB service.

Overall, we recommend transit operators reduce the number of charging events per charger. This could be addressed by selecting a larger battery size for BEBs or increasing the number/location of charging stations. Risk disruption is equally critical, which could be achieved by spreading the charging infrastructure to distribute the risk of having multiple chargers at the same location.

For scholars, it is worth noting that we presented a reactive robustness assessment of the BEB transit system. Although valid, it would be more beneficial to proactively address the BEB robustness in the optimization process by integrating robustness thresholds in the problem formulation. This item should be addressed in future research studies.

Author Contributions: Conceptualization, M.M. and H.A.; methodology, H.A. and A.F.; software, H.A. and A.F.; validation, M.M.; formal analysis, H.A. and A.F.; investigation, H.A. and A.F.; resources, M.M.; data curation, H.A.; writing—original draft preparation, H.A. and A.F..; writing—review and editing, M.M.; visualization, M.M.; supervision, M.M.; project administration, M.M.; funding acquisition, M.M. All authors have read and agreed to the published version of the manuscript.

Funding: The authors would like to acknowledge support from the Natural Sciences and Engineering Research Council of Canada (NSERC) Grant No: RGPIN-2018-05994.

Data Availability Statement: The data will be made available upon request.

Conflicts of Interest: The authors declare no conflict of interest.

Appendix A. BEB System Configuration

Table A1. Number of buses operating each hour.

Route Name	1A	1B	2A	3A	3B	4	5	6	7	8	9	10	11	12	14	15	16	20	50	56	57	58	GC	Total
Fleet Size	3	2	4	11	3	1	4	2	2	1	1	2	1	1	1	1	3	3	1	2	2	2	2	**55**
5:00 AM	0	0	1	1	0	0	1	0	0	0	1	1	1	0	0	0	1	0	0	0	0	0	0	**7**
6:00 AM	3	2	3	3	3	1	4	2	2	1	1	2	1	1	1	1	3	3	0	0	1	1	1	**40**
7:00 AM	2	2	3	5	3	1	3	1	2	1	1	0	1	1	1	0	3	2	0	0	0	0	0	**32**

Table A1. *Cont.*

Route Name	1A	1B	2A	3A	3B	4	5	6	7	8	9	10	11	12	14	15	16	20	50	56	57	58	GC	Total
8:00 AM	2	2	3	4	3	1	3	1	2	1	1	1	1	1	1	0	3	3	0	0	0	2	2	**37**
9:00 AM	2	1	3	5	3	1	4	2	2	1	1	1	1	1	1	1	2	3	1	0	0	0	0	**36**
10:00 AM	2	2	3	4	3	1	4	1	2	1	1	0	1	1	1	1	3	2	0	0	0	2	1	**36**
11:00 AM	2	2	3	4	3	1	4	2	2	1	1	2	1	1	1	1	3	2	1	2	2	2	1	**44**
12:00 PM	2	2	3	4	3	1	4	2	2	1	1	1	1	1	1	1	3	3	1	2	2	2	1	**44**
1:00 PM	2	2	3	4	3	1	4	2	2	1	1	1	1	1	1	1	3	2	1	1	1	1	1	**40**
2:00 PM	2	2	3	4	3	1	4	2	2	1	1	1	1	1	1	1	3	2	1	2	1	2	1	**42**
3:00 PM	2	2	3	5	3	1	4	2	2	1	1	2	1	1	1	1	3	2	1	1	2	2	2	**45**
4:00 PM	1	2	3	6	3	1	4	2	2	1	1	1	1	1	1	1	3	3	1	2	2	2	2	**46**
5:00 PM	0	2	3	5	3	0	3	0	2	0	1	0	1	0	0	0	3	3	0	0	0	0	0	**26**
6:00 PM	2	1	3	3	3	1	2	1	2	1	1	0	0	1	1	0	3	2	0	0	0	0	1	**28**
7:00 PM	3	2	3	4	3	1	4	2	2	1	1	2	1	1	1	1	3	3	1	2	2	2	1	**46**
8:00 PM	2	2	3	6	3	1	4	2	2	1	1	2	1	1	1	1	3	3	1	2	1	2	0	**45**
9:00 PM	2	2	3	4	3	1	4	1	2	1	1	2	1	1	1	1	3	3	1	2	2	2	0	**43**
10:00 PM	2	2	3	2	3	1	4	2	2	1	1	0	1	1	1	1	3	2	0	1	2	1	0	**36**
11:00 PM	2	2	3	3	3	1	4	2	2	1	1	2	1	1	1	1	2	2	1	1	0	0	0	**36**
12:00 AM	2	2	3	2	3	1	4	2	2	1	1	2	1	1	1	1	3	2	0	0	0	0	0	**34**
1:00 AM	0	1	2	0	2	0	2	0	0	1	0	0	0	0	0	1	1	0	0	0	1	0	0	**11**
2:00 AM	0	0	0	0	1	0	1	1	1	0	0	0	0	0	0	0	0	2	0	0	0	0	0	**6**
3:00 AM	0	0	2	0	0	0	0	1	1	0	0	1	0	0	0	0	0	1	0	0	0	0	0	**6**
4:00 AM	1	1	1	0	0	1	0	0	0	0	0	0	1	1	0	0	0	0	0	0	0	0	0	**6**
Total	**38**	**38**	**63**	**78**	**60**	**19**	**75**	**33**	**40**	**19**	**20**	**24**	**20**	**19**	**18**	**16**	**57**	**50**	**11**	**18**	**19**	**23**	**14**	**772**

Table A2. BEBs energy demand overtime for each charging station (kW at each hour).

Charging Station	1	4	7	12	13	15	19	Minimum	Maximum	Total
5:00 AM	293	293	147	147	147	147	587	147	587	3227
6:00 AM	1213	1213	527	527	527	527	1680	527	1680	11,600
7:00 AM	867	867	390	390	390	390	1187	390	1187	8307
8:00 AM	1173	1173	520	520	520	520	1600	520	1600	11,360
9:00 AM	1080	1080	487	487	487	487	1453	487	1453	10,440
10:00 AM	1093	1093	480	480	480	480	1440	480	1440	10,453
11:00 AM	1947	1947	843	843	843	843	2653	843	2653	19,093
12:00 PM	1707	1707	757	757	757	757	2427	757	2427	17,200
1:00 PM	1520	1520	667	667	667	667	2107	667	2107	14,800
2:00 PM	1720	1720	770	770	770	770	2427	770	2427	17,080
3:00 PM	1733	1733	780	780	780	780	2507	780	2507	17,787
4:00 PM	1893	1893	820	820	820	820	2667	820	2667	18,880
5:00 PM	787	787	370	370	370	370	1093	370	1093	7613
6:00 PM	800	800	360	360	360	360	1080	360	1080	7720
7:00 PM	1800	1800	787	787	787	787	2480	787	2480	17,800
8:00 PM	1973	1973	880	880	880	880	2867	880	2867	19,800
9:00 PM	1840	1840	823	823	823	823	2653	823	2653	18,587
10:00 PM	1493	1493	643	643	643	643	2067	643	2067	14,520
11:00 PM	1400	1400	633	633	633	633	1960	633	1960	13,600
12:00 AM	1347	1347	583	583	583	583	1840	583	1840	12,933
1:00 AM	440	440	217	217	217	217	733	217	733	4533
2:00 AM	240	240	120	120	120	120	480	120	480	2640
3:00 AM	187	187	93	93	93	93	373	93	373	2053
4:00 AM	307	307	153	153	153	153	613	153	613	3373
Minimum	187	187	93	93	93	93	373	93		
Maximum	1973	1973	880	880	880	880	2867		2867	
Total	28,853	28,853	12,850	12,850	12,850	12,850	40,973			285,400

Appendix B. BEB Robustness

Table A3. Service frequency under charging station hourly disruption.

Station ID / **Time of Disruption**	**1**	**1-1**	**1-2**	**4**	**4-1**	**4-2**	**4-3**	**4-4**	**7**	**12**	**13**	**15**	**19**
5:00 AM	100.00%	100.00%	100.00%	100.00%	100.00%	100.00%	100.00%	100.00%	100.00%	100.00%	100.00%	100.00%	100.00%
6:00 AM	98.64%	99.46%	99.18%	97.68%	99.05%	99.32%	99.59%	99.73%	99.25%	99.86%	**99.73%**	**99.73%**	100.00%
7:00 AM	99.18%	99.32%	99.86%	97.82%	**98.77%**	99.86%	99.46%	99.73%	99.39%	100.00%	**99.73%**	99.86%	100.00%
8:00 AM	99.05%	99.46%	99.59%	97.89%	98.84%	99.46%	99.73%	99.86%	99.39%	100.00%	99.86%	99.86%	99.32%
9:00 AM	99.05%	99.46%	99.59%	97.75%	99.11%	99.32%	99.59%	99.73%	99.46%	100.00%	**99.73%**	**99.73%**	99.80%
10:00 AM	98.77%	99.05%	99.73%	97.28%	99.18%	99.18%	99.32%	99.59%	99.52%	100.00%	99.86%	99.86%	99.52%
11:00 AM	98.09%	98.98%	**99.11%**	97.82%	99.18%	99.46%	99.59%	99.59%	99.32%	100.00%	**99.73%**	99.86%	98.84%
12:00 PM	98.09%	98.77%	99.32%	98.02%	99.39%	99.46%	99.46%	99.73%	99.52%	100.00%	**99.73%**	99.86%	98.64%
1:00 PM	98.77%	99.18%	99.59%	97.21%	98.98%	99.46%	99.32%	99.46%	99.46%	100.00%	**99.73%**	99.86%	99.39%
2:00 PM	98.57%	98.98%	99.59%	98.02%	99.39%	99.32%	99.46%	99.86%	99.39%	100.00%	**99.73%**	99.86%	99.05%
3:00 PM	98.43%	99.18%	99.25%	97.41%	99.25%	**99.11%**	99.46%	99.59%	**99.11%**	100.00%	**99.73%**	**99.73%**	98.98%
4:00 PM	97.96%	98.84%	**99.11%**	**97.14%**	99.25%	99.18%	99.39%	**99.32%**	99.25%	100.00%	**99.73%**	99.86%	98.77%
5:00 PM	99.18%	99.32%	99.86%	98.57%	99.11%	99.66%	99.80%	100.00%	99.46%	100.00%	99.86%	**99.73%**	100.00%
6:00 PM	99.32%	99.32%	100.00%	98.23%	99.32%	99.59%	99.46%	99.86%	99.59%	100.00%	99.86%	99.86%	99.86%
7:00 PM	**97.89%**	**98.77%**	**99.11%**	97.41%	99.18%	99.32%	99.46%	99.46%	99.32%	99.73%	99.86%	99.86%	**98.57%**
8:00 PM	98.16%	98.91%	99.25%	97.28%	98.91%	99.46%	**99.18%**	99.73%	99.66%	99.86%	**99.73%**	**99.73%**	98.91%
9:00 PM	98.16%	**98.77%**	99.39%	97.68%	99.05%	99.73%	99.46%	99.46%	99.52%	99.93%	**99.73%**	99.86%	98.91%
10:00 PM	98.30%	98.84%	99.46%	97.41%	99.05%	99.32%	99.46%	99.59%	99.39%	100.00%	99.86%	99.86%	99.59%
11:00 PM	98.64%	99.05%	99.59%	97.96%	**98.77%**	99.86%	99.59%	99.73%	99.52%	99.93%	99.86%	**99.73%**	100.00%
12:00 AM	99.18%	99.52%	99.66%	98.84%	99.52%	99.80%	99.66%	99.86%	99.86%	**99.66%**	99.93%	99.93%	100.00%
1:00 AM	100.00%	100.00%	100.00%	100.00%	100.00%	100.00%	100.00%	100.00%	100.00%	100.00%	100.00%	100.00%	100.00%
2:00 AM	NA	NA	NA	NA	NA	NA	NA	NA	NA	NA	NA	NA	NA
3:00 AM	NA	NA	NA	NA	NA	NA	NA	NA	NA	NA	NA	NA	NA
4:00 AM	NA	NA	NA	NA	NA	NA	NA	NA	NA	NA	NA	NA	NA
5:00 AM–next day	NA	NA	NA	NA	NA	NA	NA	NA	NA	NA	NA	NA	NA

References

1. Xiong, J.; Bai, C.; Guan, W.; Chen, Y.; Xu, Y. Mixed Optimization on Vehicle Scheduling and Recharge Scheduling of Plug-In Electric Buses with Consideration of Partial Recharge. *J. Transp. Eng. Part A Syst.* **2022**, *148*, 04021111. [CrossRef]
2. He, Y.; Song, Z.; Liu, Z. Fast-charging station deployment for battery electric bus systems considering electricity demand charges. *Sustain. Cities Soc.* **2019**, *48*, 101530. [CrossRef]
3. Soukhov, A.; Mohamed, M. Occupancy and GHG emissions: Thresholds for disruptive transportation modes and emerging technologies. *Transp. Res. Part D Transp. Environ.* **2022**, *102*, 103127. [CrossRef]
4. Mahmoud, M.; Garnett, R.; Ferguson, M.; Kanaroglou, P. Electric buses: A review of alternative powertrains. *Renew. Sust. Energ. Rev.* **2016**, *62*, 673–684. [CrossRef]
5. Foda, A.; Mohamed, M.; Bakr, M. Dynamic Surrogate Trip-Level Energy Model for Electric Bus Transit System Optimization. *Transp. Res. Rec. J. Transp. Res. Board* **2022**, *2677*, 513–528. [CrossRef]
6. El-Taweel, N.A.; Farag, H.E.Z.; Mohamed, M. Integrated Utility-Transit Model for Optimal Configuration of Battery Electric Bus Systems. *IEEE Syst. J.* **2020**, *14*, 738–748. [CrossRef]
7. Liu, Z.; Song, Z.; He, Y. Economic Analysis of On-Route Fast Charging for Battery Electric Buses: Case Study in Utah. *Transp. Res. Rec. J. Transp. Res. Board* **2019**, *2673*, 119–130. [CrossRef]
8. Rogge, M.; van der Hurk, E.; Larsen, A.; Sauer, D.U. Electric bus fleet size and mix problem with optimization of charging infrastructure. *Appl. Energy* **2018**, *211*, 282–295. [CrossRef]
9. Abdelaty, H.; Al-Obaidi, A.; Mohamed, M.; Farag, H.E.Z. Machine learning prediction models for battery-electric bus energy consumption in transit. *Transp. Res. Part D-Transp. Environ.* **2021**, *96*, 102868. [CrossRef]
10. Pamuła, T.; Pamuła, W. Estimation of the Energy Consumption of Battery Electric Buses for Public Transport Networks Using Real-World Data and Deep Learning. *Energies* **2020**, *13*, 2340. [CrossRef]
11. Vepsäläinen, J.; Kivekäs, K.; Otto, K.; Lajunen, A.; Tammi, K. Development and validation of energy demand uncertainty model for electric city buses. *Transp. Res. Part D Transp. Environ.* **2018**, *63*, 347–361. [CrossRef]
12. Liu, X.; Qu, X.; Ma, X. Optimizing electric bus charging infrastructure considering power matching and seasonality. *Transp. Res. Part D Transp. Environ.* **2021**, *100*, 103057. [CrossRef]
13. An, K. Battery electric bus infrastructure planning under demand uncertainty. *Transp. Res. Part C Emerg. Technol.* **2020**, *111*, 572–587. [CrossRef]
14. Liu, K.; Yamamoto, T.; Morikawa, T. Impact of road gradient on energy consumption of electric vehicles. *Transp. Res. Part D: Transp. Environ.* **2017**, *54*, 74–81. [CrossRef]
15. Perrotta, D.; Macedo, J.L.; Rossetti, R.J.F.; Sousa, J.F.d.; Kokkinogenis, Z.; Ribeiro, B.; Afonso, J.L. Route Planning for Electric Buses: A Case Study in Oporto. *Procedia-Soc. Behav. Sci.* **2014**, *111*, 1004–1014. [CrossRef]
16. Wei, R.; Liu, X.; Ou, Y.; Kiavash Fayyaz, S. Optimizing the spatio-temporal deployment of battery electric bus system. *J. Transp. Geogr.* **2018**, *68*, 160–168. [CrossRef]
17. Uslu, T.; Kaya, O. Location and capacity decisions for electric bus charging stations considering waiting times. *Transp. Res. Part D Transp. Environ.* **2021**, *90*, 102645. [CrossRef]
18. Rupp, M.; Rieke, C.; Handschuh, N.; Kuperjans, I. Economic and ecological optimization of electric bus charging considering variable electricity prices and CO2eq intensities. *Transp. Res. Part D Transp. Environ.* **2020**, *81*, 102293. [CrossRef]
19. Kunith, A.; Mendelevitch, R.; Goehlich, D. Electrification of a city bus network—An optimization model for cost-effective placing of charging infrastructure and battery sizing of fast-charging electric bus systems. *Int. J. Sustain. Transp.* **2017**, *11*, 707–720. [CrossRef]
20. Gormez, M.A.; Topcu, A.; Sozer, Y. Cost Optimization of an Opportunity Charging Bus Network. In Proceedings of the 2018 IEEE Energy Conversion Congress and Exposition (ECCE), Portland, OR, USA, 23–27 September 2018; pp. 2782–2789.
21. Zhou, Y.; Liu, X.C.; Wei, R.; Golub, A. Bi-Objective Optimization for Battery Electric Bus Deployment Considering Cost and Environmental Equity. *IEEE Trans. Intell. Transp. Syst.* **2021**, *22*, 2487–2497. [CrossRef]
22. Bi, Z.; Keoleian, G.A.; Ersal, T. Wireless charger deployment for an electric bus network: A multi-objective life cycle optimization. *Appl. Energy* **2018**, *225*, 1090–1101. [CrossRef]
23. Alwesabi, Y.; Avishan, F.; Yanıkoğlu, İ.; Liu, Z.; Wang, Y. Robust strategic planning of dynamic wireless charging infrastructure for electric buses. *Appl. Energy* **2022**, *307*, 118243. [CrossRef]
24. Liu, K.; Gao, H.; Wang, Y.; Feng, T.; Li, C. Robust charging strategies for electric bus fleets under energy consumption uncertainty. *Transp. Res. Part D Transp. Environ.* **2022**, *104*, 103215. [CrossRef]
25. Liu, Z.; Song, Z.; He, Y. Planning of Fast-Charging Stations for a Battery Electric Bus System under Energy Consumption Uncertainty. *Transp. Res. Rec. J. Transp. Res. Board* **2018**, *2672*, 96–107. [CrossRef]
26. Zheng, F.; Wang, Z.; Liu, M. Overnight charging scheduling of battery electric buses with uncertain charging time. *Oper. Res.* **2022**, *22*, 4865–4903. [CrossRef]
27. Iliopoulou, C.; Kepaptsoglou, K. Robust electric transit route network design problem (RE-TRNDP) with delay considerations: Model and application. *Transp. Res. Part C Emerg. Technol.* **2021**, *129*, 103255. [CrossRef]
28. Eldeeb, G.; Mohamed, M. Transit electrification state of the art: A machine-learning based text mining approach. *Transp. Res. Part D Transp. Environ.* **2022**, *111*, 103446. [CrossRef]

29. Xu, Z.; Zhang, C.; Chopra, S.S. Robustness assessment of public bus transit system with a response-integrated approach for a resilient public transport system in Hong Kong. *Transp. B Transp. Dyn.* **2022**, 1–15. [CrossRef]
30. Jia, T.; Liu, W.; Liu, X. A cross-city exploratory analysis of the robustness of bus transit networks using open-source data. *Phys. A Stat. Mech. Its Appl.* **2021**, *580*, 126133. [CrossRef]
31. Abdelaty, H.; Mohamed, M.; Ezzeldin, M.; El-Dakhakhni, W. Quantifying and classifying the robustness of bus transit networks. *Transp. A Transp. Sci.* **2020**, *16*, 1176–1216. [CrossRef]
32. Barabási, A.L.; PÃ3sfai, M.Ã. *Network Science*; Cambridge University Press: Cambridge, UK, 2016.
33. Li, M.; Tang, P.; Lin, X.; He, F. Multistage planning of electric transit charging facilities under build-operate-transfer model. *Transp. Res. Part D Transp. Environ.* **2022**, *102*, 103118. [CrossRef]
34. Benoliel, P.; Jenn, A.; Tal, G. Examining energy uncertainty in battery bus deployments for transit agencies in California. *Transp. Res. Part D Transp. Environ.* **2021**, *98*, 102963. [CrossRef]
35. Wu, X.; Feng, Q.; Bai, C.; Lai, C.S.; Jia, Y.; Lai, L.L. A novel fast-charging stations locational planning model for electric bus transit system. *Energy* **2021**, *224*, 106. [CrossRef]
36. Lotfi, M.; Pereira, P.; Paterakis, N.; Gabbar, H.A.; Catalão, J.P.S. Optimizing Charging Infrastructures of Electric Bus Routes to Minimize Total Ownership Cost. In Proceedings of the 2020 IEEE International Conference on Environment and Electrical Engineering and 2020 IEEE Industrial and Commercial Power Systems Europe (EEEIC/I&CPS Europe), Madrid, Spain, 9–12 June 2020; pp. 1–6.
37. Lin, Y.; Zhang, K.; Shen, Z.-J.M.; Ye, B.; Miao, L. Multistage large-scale charging station planning for electric buses considering transportation network and power grid. *Transp. Res. Part C Emerg. Technol.* **2019**, *107*, 423–443. [CrossRef]
38. Wang, Y.; Huang, Y.; Xu, J.; Barclay, N. Optimal recharging scheduling for urban electric buses: A case study in Davis. *Transp. Res. Part E Logist. Transp. Rev.* **2017**, *100*, 115–132. [CrossRef]
39. Bie, Y.; Ji, J.; Wang, X.; Qu, X. Optimization of electric bus scheduling considering stochastic volatilities in trip travel time and energy consumption. *Comput.-Aided Civ. Infrastruct. Eng.* **2021**, *36*, 1530–1548. [CrossRef]
40. Zhou, Y.; Wang, H.; Wang, Y.; Li, R. Robust optimization for integrated planning of electric-bus charger deployment and charging scheduling. *Transp. Res. Part D Transp. Environ.* **2022**, *110*, 103410. [CrossRef]
41. Jiang, M.; Zhang, Y.; Zhang, Y.; Li, W. Optimal Electric Bus Scheduling under Travel Time Uncertainty: A Robust Model and Solution Method. *J. Adv. Transp.* **2021**, *2021*, 1–19. [CrossRef]
42. Hu, H.; Du, B.; Liu, W.; Perez, P. A joint optimisation model for charger locating and electric bus charging scheduling considering opportunity fast charging and uncertainties. *Transp. Res. Part C Emerg. Technol.* **2022**, *141*, 103732. [CrossRef]
43. Tessler, M.E.; Traut, E.J. Hurricane resiliency methods for the New York City electric bus fleet. *Transp. Res. Part D Transp. Environ.* **2022**, *105*, 103255. [CrossRef]
44. Wang, Y.; Liao, F.; Lu, C. Integrated optimization of charger deployment and fleet scheduling for battery electric buses. *Transp. Res. Part D Transp. Environ.* **2022**, *109*, 103382. [CrossRef]
45. Liu, K.; Gao, H.; Liang, Z.; Zhao, M.; Li, C. Optimal charging strategy for large-scale electric buses considering resource constraints. *Transp. Res. Part D Transp. Environ.* **2021**, *99*, 103009. [CrossRef]
46. Darby-Dowman, K.; Wilson, J.M. Developments in linear and integer programming. *J. Oper. Res. Soc.* **2017**, *53*, 1065–1071. [CrossRef]
47. Genova, K.; Guliashki, V. Linear integer programming methodsand approaches—A survey. *Cybern. Inf. Technol.* **2011**, *11*, 3–25.
48. Kuma, P.H.; Mageshvaran, R. Methods And Solvers Used For Solving Mixed Integer Linear Programming And Mixed Nonlinear Programming Problems: A Review. *Int. J. Sci. Technol. Res.* **2020**, *9*, 1872–1882.
49. Albert, R.; Barabási, A.-L. Statistical mechanics of complex networks. *Rev. Mod. Phys.* **2002**, *74*, 47–97. [CrossRef]
50. Remix. Base Network_Hamilton Bus Transit Network. Available online: https://platform.remix.com/?explore=true&latlng=43.13105,-79.68847,8.061&layer=simple (accessed on 5 January 2023).
51. Guelph_Schedule. Available online: https://transitfeeds.com/p/guelph-transit/53 (accessed on 23 December 2022).
52. Lin, Y.; Zhang, K.; Shen, Z.-J.M.; Miao, L. Charging Network Planning for Electric Bus Cities: A Case Study of Shenzhen, China. *Sustainability* **2019**, *11*, 4713. [CrossRef]
53. Sobol, I.M. Sensitivity Estimates for Nonlinear Mathematical Models. *Math. Model. Comput. Exp.* **1993**, *4*, 407–414.
54. Sobol, I.M. On the distribution of points in a cube and the approximate evaluation of integrals. *USSR Comput. Math. Math. Phys.* **1967**, *7*, 86–112. [CrossRef]
55. Saltelli, A.; Ratto, M.; Andres, T.; Campolongo, F.; Cariboni, J.; Gatelli, D.; Saisana, M.; Tarantola, S. Sensitivity Analysis: From Theory to Practice. In *Global Sensitivity Analysis. The Primer*; John Wiley & Sons, Ltd.: Hoboken, NJ, USA, 2007; Volume 1, pp. 237–275.